THE JOURNAL OF PHYSICAL CHEMISTRY B

Article

pubs.acs.org/JPCB

Hydrophilic and Hydrophobic Hydration of Sodium Propanoate and Sodium Butanoate in Aqueous Solution

Hafiz M. A. Rahman,[†] Glenn Hefter,[‡] and Richard Buchner*[,†]

[†]Institut für Physikalische und Theoretische Chemie, Universität Regensburg, D-93040 Regensburg, Germany

[‡]Chemistry Department, Murdoch University, Murdoch, WA 6150 Australia

Supporting Information

ABSTRACT: Aqueous solutions of sodium propanoate (NaOPr) and *n*-butanoate (NaOBu) have been studied at concentrations of $c \lesssim 3$ M by broadband dielectric relaxation spectroscopy over the frequency range $0.2 \leq \nu/\mathrm{GHz} \leq 89$ at 25 °C. Three relaxation modes were resolved, centered at (approximately) 1, 8, and 18 GHz, for both sets of solutions. The two faster modes were assigned to the cooperative relaxation of "slow" and bulk water molecules. Detailed analysis of the spectra indicated that both OPr^- and OBu^- were strongly hydrated, with ~23 and ~33 slow water molecules per anion, respectively, at infinite dilution. These effective hydration numbers include ~6 water molecules hydrophilically bound to the carboxylate moiety, with the remainder arising from the hydrophobic hydration of the nonpolar alkyl chains. The latter shows a characteristic rapid decrease with increasing solute concentration, which facilitated the separation of the hydrophobic and hydrophilic contributions. The lowest frequency mode was a composite with contributions from ion-cloud, ion-pair, and anion relaxations. Although this low intensity mode provided specific evidence of weak ion pairing between $Na^+(aq)$ and the carboxylate anions, reliable estimates of the association constant could not be made because of its composite nature.

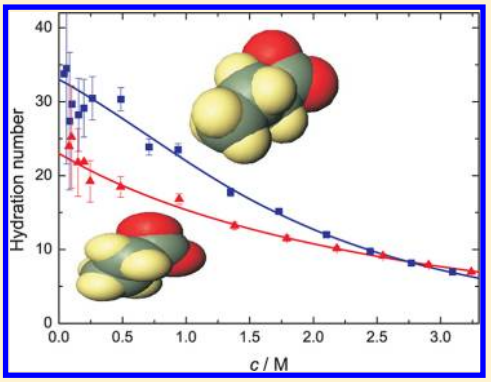

1. INTRODUCTION

The significance of hydration processes is overwhelming and accordingly these have been investigated intensively.[1−5] An important finding from these studies is that many solutes contain both hydrophilic and hydrophobic components and that especially for biomolecules but also for many small molecules of technical importance the interaction of these very different attributes plays a significant role in their function. Hydrophobic hydration is mostly associated with the hydrocarbon constituents of the molecular structure while hydrophilic (nucleophilic and electrophilic) interactions with water are dominated by electron donor/acceptor atoms and any positively or negatively charged groups present.[6,8] A known (and especially for biomolecule solutions important) but less well understood aspect of this picture is that changes in the structure of adjacent solvent layers wrought by the presence of a molecule can in turn interact with that molecule, further influencing its structure and activity.[6]

Unfortunately, the study of molecular hydration is greatly complicated by the similarity of the time scales of the dynamics of H_2O molecules in the solute solvation sheath and in the bulk solvent, creating difficulties for almost all techniques.[3,5,7] This problem can be side-stepped to some extent by studying appropriate model compounds which are within the reach of computer simulations[9,10] and scattering methods;[11,12] nevertheless the information that can be obtained is still rather limited.

Of the various model species that possess both hydrophilic and hydrophobic components, perhaps the simplest are the alkylcarboxylate ions, $RCOO^-$, which contain just one hydrocarbon and one hydrophilic moiety. The hydrophilic carboxylate group is a particularly important component of many technically and/or biologically relevant molecules being found, for example, in amino acids, fatty acids, lipid bilayers and surface-active agents.[13] Another key aspect of carboxylates is their interaction with cations. This feature is of special interest because carboxylate moieties are present at many of the active sites of enzymes, where they are thought to perform a metal-ion binding function,[14] and because of their effect on protein association. Not surprisingly, carboxylate hydration has been intensively studied with computer simulations,[9,15] NMR[16] and IR spectroscopy,[6,17] and X-ray and neutron scattering techniques.[18,19] However, these studies were mostly focused on the hydration of the $-COO^-$ group and only to a lesser degree on the effects of their alkyl substituents.

Although considerable advances have been made in understanding the hydration of solutes combining hydrophilic and hydrophobic moieties, there are still many issues yet to be resolved. For example, it has been claimed[6] on the basis of IR spectroscopy that water molecules surrounding nonpolar substituents of solute species are spectrally equivalent to

Received: October 10, 2012
Revised: January 24, 2013
Published: January 24, 2013

dx.doi.org/10.1021/jp310029c | J. Phys. Chem. B 2013, 117, 2142−2152

those in the bulk phase. Likewise, the ion-pairing interactions of carboxylates with the alkali metal ions are far from well understood even though, for example, computer simulations[20,21] suggest that they may be critical for understanding protein function. The interaction of $Na^+(aq)$ with carboxylate moieties is of special interest.[20,21] Not only is $Na^+(aq)$ ubiquitous, and frequently the dominant ion, in biological solutions, but its control and transport are critical in many biological functions. However, these interactions are typically weak and strongly affected by hydration and so are particularly hard to quantify.

Broadband dielectric relaxation spectroscopy (DRS), which probes the response of dipolar species to a time-dependent electric field in the microwave region, is a powerful tool for the study of the hydration of solutes and the effects of those solutes on the cooperative dynamics of bulk water.[22,23] DRS is also one of the few techniques available that can quantify the formation of weak ion pairs and also determine their level of hydration.[22] Previous DRS measurements of aqueous solutions of the smallest sodium carboxylate salts: formate (NaOOCH, NaOFm) and acetate ($NaOOCCH_3$, NaOAc), revealed several interesting features about their hydration.[8] In particular it was shown that the carboxylate group immobilizes ("irrotationally binds") almost no H_2O molecules yet is hydrated strongly enough to measurably slow the dynamics of ∼5.2 H_2O molecules per $-COO^-$. Somewhat unexpectedly, it was found that the methyl group in OAc^- also exhibited a significant level of hydrophobic hydration.

To gain a deeper understanding of the interplay of hydrophilic and hydrophobic hydration in species possessing both characteristics, this paper presents a detailed broadband DRS study of the aqueous solutions of sodium propanoate ($NaOOCCH_2CH_3$, NaOPr) and sodium *n*-butanoate ($NaOOC(CH)_2CH_3$, NaOBu) up to high concentrations and over the frequency range from ∼0.2 to 89 GHz at 25 °C. (Note that the abbreviations adopted here for these ions are merely a convenient shorthand; strictly speaking they should be written as the more cumbersome $EtCOO^-$ and *n*-$PrCOO^-$, respectively.)

2. EXPERIMENTAL SECTION

Sodium propanoate (purity ≥99%) and sodium butanoate (purity ≥98%) were obtained from Fluka (Steinheim, Germany) and Merck (Hohenbrunn, Germany), respectively. Both salts were dried at 60 °C under high vacuum (∼10^{-5} bar) for at least 72 h using P_2O_5 (Sicapent, Merck) as a desiccant and were stored in a nitrogen-filled glovebox before use. Aqueous solutions were prepared gravimetrically without buoyancy corrections using degassed high purity (Millipore Milli-Q) water. However, for data processing purposes, all concentrations, *c*, are expressed in M (mol solute)/(L solution).

Solution densities, ρ, required for the conversion from gravimetric to volumetric units were determined at 25 ± 0.01 °C with an accuracy of ±0.05 kg m^{-3} using a vibrating-tube densimeter (Anton Paar DMA 60) calibrated with $N_2(g)$ and water, assuming densities from standard sources.[24] Electrical conductivities, κ, were measured at 25 ± 0.005 °C, over the frequency range $0.1 \leq \nu/\text{kHz} \leq 10$ with an accuracy of ±0.5%, using an AC bridge and capillary cells as described elsewhere.[25] To eliminate electrode polarization, the conductivity of each sample was obtained as $\kappa = C/R_\infty$ where R_∞ ($= \lim_{\nu\to\infty} R(\nu)$) was obtained by extrapolation using the empirical function $R(\nu) = R_\infty + A/\nu^a$, where *A*, which is specific to the cell, and *a* ≈ 0.5 are empirical parameters.[25]

Dielectric spectra of NaOPr(aq) at 25 °C were recorded at Murdoch University in the frequency range $0.2 \leq \nu/\text{GHz} \leq 20$ using a Hewlett-Packard model 85070 M dielectric probe system based on a HP 8720D vector network analyzer (VNA), as described previously.[26] Temperature was controlled by a Hetofrig (Denmark) circulator-thermostat with an accuracy of ±0.05 °C. Dielectric spectra of NaOBu(aq) at 25 °C were recorded at Regensburg University in the frequency range $0.2 \leq \nu/\text{GHz} \leq 50$ with an Agilent E8364B vector network analyzer connected to an electronic calibration module (Ecal, Agilent N4693A) and a dielectric probe kit (85070E). Two different commercial open-ended coaxial probes, a "high temperature" probe in the frequency range $0.2 \leq \nu/\text{GHz} \leq 20$ and a "performance" probe in the frequency range $1 \leq \nu/\text{GHz} \leq 50$, were used at 61 and 51 separate frequencies equidistant on a logarithmic scale, respectively. The data from the performance probe, however, were used only at $15 \lesssim \nu/\text{GHz} \leq 50$ in the fitting procedure so as to maintain an equal density of data points throughout the frequency range. All VNA spectra were recorded at least twice using independent calibrations with air, water, and mercury as the references. Higher frequency data were also recorded at Regensburg using two interferometers: A-band ($27 \leq \nu/\text{GHz} \leq 39$) and E-band ($60 \leq \nu/\text{GHz} \leq 89$). The operation of these instruments is described in detail elsewhere.[27] Temperature control and accuracy for both the network analyzer and interferometric measurements were similar to those at Murdoch. Typical spectra and the corresponding fits are shown in Figures 1 and 2.

3. DATA ANALYSIS

Dielectric spectroscopy records the total polarization, $\vec{P}(t)$, of a sample in a time-dependent field, $\vec{E}(t)$, as a function of the field frequency, ν. The measured quantity is the overall complex permittivity $\hat{\eta}(\nu) = \eta'(\nu) - i\eta''(\nu)$, but for discussion purposes, the sample response is usually expressed in terms of the complex permittivity:

$$\hat{\varepsilon}(\nu) = \varepsilon'(\nu) - i\varepsilon''(\nu) \tag{1}$$

where

$$\varepsilon'(\nu) = \eta'(\nu) \text{ and } \varepsilon''(\nu) = \eta''(\nu) - \frac{\kappa}{2\pi\nu e_0} \tag{2}$$

In eq 2, κ is the dc conductivity of the solution and ε_0 the permittivity of free space. The relative permittivity, $\varepsilon'(\nu)$, shows a dispersion from the static permittivity limit at low frequency, ε, to the high-frequency limit, ε_∞. The dielectric loss, $\varepsilon''(\nu)$, expresses the energy dissipation within the sample, arising from the coupling of $\vec{E}(t)$ to dipole fluctuations, whereas κ characterizes the stationary (diffusive) charge transport. Note that $\hat{\varepsilon}(\nu)$ contains all of the contributions to $\vec{P}(t)$ that depend on frequency, irrespective of their rotational, vibrational, or translational character.

The value of κ for the solutions can be determined, in principle, either from conventional low-frequency conductance measurements[28] or as an additional parameter in the fitting of the DRS data. In practice fitted κ values deviate slightly from directly measured values due to field imperfections that arise from the geometry of the VNA probe.[29] Accordingly, experimental κ values were chosen as a starting approximation in the fitting procedure but were generally 1 - 2% greater than the fitted values used. Averaged VNA spectra were combined

dx.doi.org/10.1021/jp310029c | J. Phys. Chem. B 2013, 117, 2142−2152

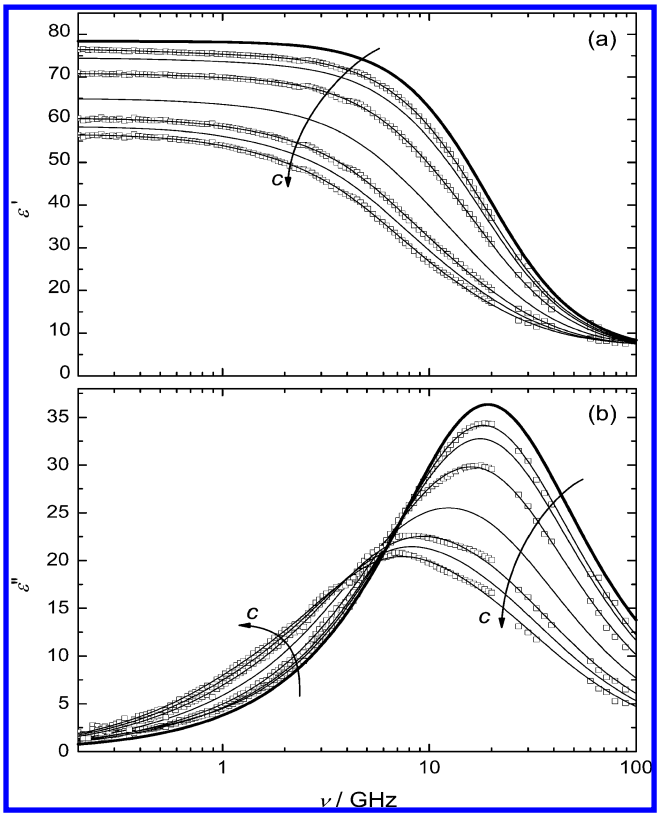

Figure 1. Dielectric permittivity (a) and loss (b) spectra for NaOPr(aq) at 25 °C and solute concentrations: c/M = 0.2978, 0.4862, 0.9452, 1.792, 2.548, 2.906, and 3.241. Arrows indicate increasing concentration; symbols are randomly selected experimental data (others are omitted for visual clarity); lines represent the D+D+D fit; heavy lines denote the pure water spectra.

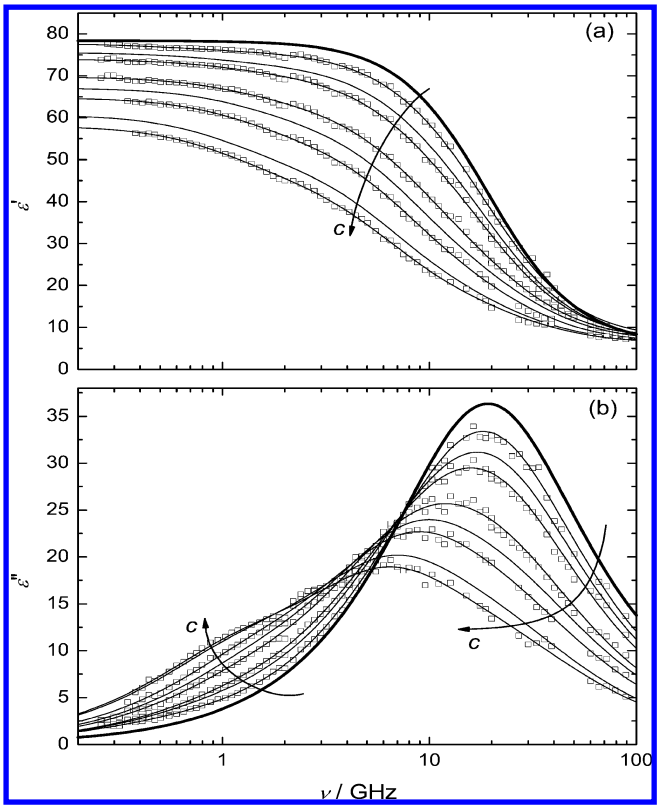

Figure 2. Dielectric permittivity (a) and loss (b) spectra for NaOBu(aq) at 25 °C and solute concentrations: c/M = 0.1962, 0.4867, 0.7080, 1.349, 1.729, 2.104, 2.770, and 3.094. Arrows indicate increasing concentration; symbols are randomly selected experimental data (others are omitted for visual clarity); lines represent the D+D+D fit; heavy lines denote the pure water spectra.

with interferometer data. There was, in general, a good fit between the low and high frequency data (Figures 1 and 2) although, as is usually observed for electrolyte solutions, the noise increased with increasing solute concentration.[26,28]

For the formal description of the spectra, various models based on the sum of n individual relaxation processes

$$\hat{\varepsilon}(\nu) = \varepsilon_\infty + \sum_{j=1}^{n} \frac{\varepsilon_j - \varepsilon_{j+1}}{[1 + (i2\pi\nu\tau_j)^{1-\alpha_j}]^{\beta_j}} \quad (3)$$

were tested using a nonlinear least-squares routine that simultaneously fitted the in-phase ($\varepsilon'(\nu)$, Figures 1a and 2a) and out-of-phase ($\varepsilon''(\nu)$, Figures 1b and 2b) components. Each dispersion step j, of amplitude $S_j = \varepsilon_j - \varepsilon_{j+1}$, was modeled by a Havriliak–Negami (HN) equation with relaxation-time distribution parameters $0 < \alpha_j < 1$ and $0 < \beta_j \leq 1$. The simplified variants of this equation are the Cole–Davidson (CD, $\alpha_j = 0$), Cole–Cole (CC, $\beta_j = 1$), or Debye (D, $\alpha_j = 0$, $\beta_j = 1$) equations.[30,31] Other band-shape functions more appropriate for intermolecular vibrations and librations, such as a damped harmonic oscillator, were not considered as such modes contribute to the dielectric spectra of aqueous systems only at much higher frequencies.[32]

To evaluate the quality of the fit, the reduced error function[33]

$$\chi_r^2 = \frac{1}{2N - m - 1}\left[\sum_{k=1}^{N} \delta\varepsilon'(\nu_k)^2 + \sum_{k=1}^{N} \delta\varepsilon''(\nu_k)^2\right] \quad (4)$$

was calculated, where $\delta\varepsilon'(\nu_k)$ and $\delta\varepsilon''(\nu_k)$ are the residuals, N is the number of data triples $[\nu_k, \varepsilon'(\nu_k), \varepsilon''(\nu_k)]$, and m the number of the adjustable parameters. No weighting was used. Note that because of the nonlinear nature of the fitting procedure, it is not possible to assign statistically meaningful standard uncertainties to the individual fit parameters.[33] The preferred model was that which gave the lowest value of χ_r^2 and relaxation amplitudes and times that were physically realistic and varied smoothly with solute concentration.

In eq 3, $\varepsilon_\infty = \varepsilon_{n+1}$ is the infinite-frequency permittivity which in principle reflects contributions only from intramolecular polarizability. Its determination requires experiments in the far-infrared at frequencies where the contributions from molecular librations are negligible.[31,34] However, this part of the electromagnetic spectrum is difficult to access experimentally and ε_∞ is commonly treated, as in this investigation, as an adjustable parameter. The static relative permittivity of the sample is defined as $\varepsilon = \varepsilon_1 = \sum S_j + \varepsilon_\infty$. All fitting parameters are summarized in Tables 1 and 2. Additionally, randomly selected spectra were analyzed with a procedure[35] that allows an "unbiased" determination of the number of relaxation processes required for formal description of $\hat{\varepsilon}(\nu)$. Typical results from these analyses are given in the Supporting Information, Figures S1 and S2.

It was found that a sum of three Debye modes (n = 3, a D+D+D model) provided the best fit for the spectra at all studied concentrations of NaOPr(aq) and NaOBu(aq). No fast water mode centered at ~0.4 ps, often but not always observed in aqueous electrolyte solutions,[32] could be resolved for the

dx.doi.org/10.1021/jp310029c | J. Phys. Chem. B 2013, 117, 2142–2152

Table 1. Densities, ρ, Electrical Conductivities, κ, Limiting Permittivities, ε_j, Relaxation Times, τ_j, and Reduced Error Function Values, χ_r^2, for NaOPr(aq) at Concentrations, c, and 25 °C[a]

c	ρ	κ	ε	τ_1	ε_2	τ_2[b]	ε_3	τ_3[b]	ε_∞	χ_r^2
0[c]			78.37					8.32	3.48	0.048
0.07956	1.0005	0.568	79.06	832	77.44	16.2	74.85	8.28	5.50	0.064
0.09920	1.0014	0.694	78.97	749	77.26	16.2	73.87	8.28F	5.66	0.013
0.1496	1.0034	0.997	78.88	703	76.77	17.0F	72.36	8.29	5.72	0.048
0.1973	1.0053	1.28	78.01	535	76.27	17.0	70.44	8.25F	5.77	0.017
0.2459[d]	1.0073	1.55	77.07	356	75.78	16.6	69.38	8.24F	5.57	0.012
0.2978	1.0096	1.84	76.58	301	75.31	17.2	69.22	8.38	5.84	0.041
0.4862	1.0172	2.68	74.47	200	73.51	17.0	61.37	8.13	5.73	0.062
0.9452	1.0356	4.26	70.87	212	69.85	17.9	48.36	7.89	5.98	0.050
1.380[d]	1.0527	5.24	67.71	209	66.56	20.1	41.92	7.94F	6.18	0.051
1.792	1.0685	5.87	64.96	165	63.40	21.2	35.54	7.96	6.46	0.064
2.184[d]	1.0835	6.22	62.60	157	60.48	22.7	30.59	7.70F	6.13	0.058
2.548	1.0967	6.34	60.33	124	57.14	23.2	25.71	7.53	6.54	0.059
2.906	1.1096	6.23	58.40	121	54.26	24.5	23.21	7.74	6.72	0.064
3.241	1.1216	6.21	56.59	119	51.39	25.6	20.92	7.81	6.87	0.066

[a]Units: c in M; ρ in kg L^{-1}; κ in Ω^{-1} m^{-1}; τ_j in 10^{-12} s. [b]Parameter values followed by the letter F were held constant (fixed) during the fitting procedure. [c]Reference 38. [d]VNA (0.2−20 GHz) data only.

Table 2. Densities, ρ, Electrical Conductivities, κ, Limiting Permittivities, ε_j, Relaxation Times, τ_j, and Reduced Error Function Values, χ_r^2, for NaOBu(aq) at Concentrations, c, and 25 °C[a]

c	ρ	κ	ε	τ_1	ε_2	τ_2	ε_3	τ_3[b]	ε_∞	χ_r^2
0[c]			78.37					8.32	3.48	0.048
0.02299	0.9980	0.172	79.01	1153	77.84	25.2	76.58	8.32F	6.46	0.111
0.04043	0.9986	0.302	78.84	845	77.63	24.4	75.78	8.32F	6.52	0.159
0.05948	0.9994	0.380	78.71	640	77.45	22.4	74.68	8.32F	6.82	0.208
0.08271	1.0003	0.564	78.90	644	77.24	25.0	74.18	8.32F	7.20	0.259
0.1032	1.0012	0.655	78.52	490	76.99	22.3	72.84	8.32F	7.08	0.302
0.1549	1.0032	0.976	78.04	326	76.37	20.2	70.46	8.32F	7.04	0.297
0.1962	1.0049	1.23	77.67	268	75.89	19.7	68.16	8.20F	7.13	0.321
0.2632	1.0075	1.60	77.27	249	75.23	19.2	64.39	8.00F	6.70	0.228
0.4867	1.0164	2.57	75.57	167	72.75	17.3	52.78	7.56	6.45	0.218
0.7080	1.0250	3.35	73.94	140	70.43	18.3	47.59	7.56	6.81	0.229
0.9368	1.0338	3.97	72.47	134	67.91	17.8	38.13	6.90	6.58	0.206
1.349	1.0493	4.62	69.74	121	63.32	18.7	30.94	6.76	7.01	0.209
1.729	1.0634	5.04	67.11	113	58.89	19.1	23.49	5.76	6.56	0.207
2.104	1.0768	5.20	64.75	116	54.49	20.0	20.39	5.90F	6.24	0.178
2.447	1.0884	5.22	62.69	130	51.69	22.4	19.44	5.98	6.12	0.144
2.770	1.0988	5.17	60.71	143	48.61	23.9	18.03	6.37	6.33	0.162
3.094	1.1085	5.04	58.07	145	45.12	24.6	15.99	5.86	6.09	0.174

[a]Units: c in M; ρ in kg L^{-1}; κ in Ω^{-1} m^{-1}; τ_j in 10^{-12} s. [b]Parameter values followed by the letter F were held constant (fixed) during the fitting procedure. [c]Reference 38.

present samples but the fitted values of $\varepsilon_\infty \approx 5.5$ - 7.0 (Tables 1 and 2) suggest its presence.

4. RESULTS AND DISCUSSION

4.1. Relaxation Modes. The DR spectra obtained for NaOPr(aq) and NaOBu(aq) as a function of solute concentration (Figures 1 and 2) are at first glance broadly similar but in fact show significant differences. For example, the $\varepsilon''(\nu)$ curves for NaOBu(aq) show a greater decrease than NaOPr(aq) in the amplitude of the dominant peak centered at ~18 GHz and a larger increase in amplitude at frequencies around ~1 GHz with increasing solute concentration. Nevertheless, both sets of spectra were well described by a three-Debye-process (D+D+D) model. It should of course be kept in mind that a good fit of $\hat{\varepsilon}(\nu)$ with any band-shape model does not guarantee that the model is physically meaningful. The physical reasonableness of the models used is founded on the interpretation of the derived parameters and their variation with solute concentration as well as their agreement with independent information from other techniques.[36] For both sets of salt solutions the observed modes were centered (approximately) at 1, 8, and 20 GHz (Figures 3 and 4). For reasons that will be discussed in detail below they are labeled "IP + IC + X^-" (or just "X^-", see Section 4.2) for the slowest (j = 1) process, "slow H_2O" for the intermediate frequency (j = 2) process and "bulk H_2O" for the highest frequency (j = 3) process.

4.2. Relaxation Times. *Bulk Water.* The relaxation time, $\tau_3(c) = \tau_b$, of the highest frequency mode, centered at ~18 GHz in the DR spectra of both NaOPr(aq) (Figure 3) and NaOBu(aq) (Figure 4), smoothly extrapolates (Figure 5) to that of the dominant bulk (subscript b) mode in pure water,

dx.doi.org/10.1021/jp310029c | J. Phys. Chem. B 2013, 117, 2142−2152

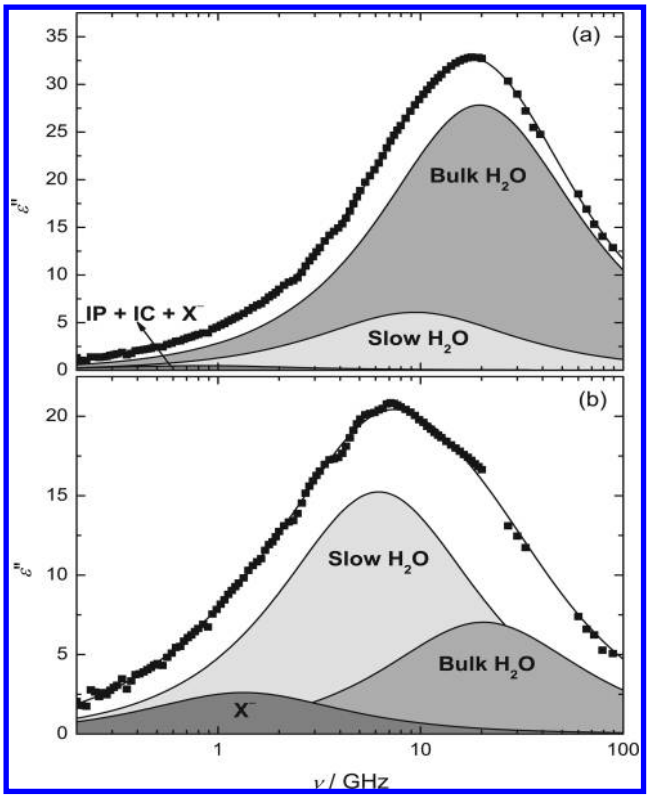

Figure 3. Dielectric loss curve of (a) 0.4862 M and (b) 3.241 M NaOPr(aq) at 25 °C, showing the contributions of the three Debye processes. Symbols represent experimental data, lines represent the D +D+D fit, and shaded areas indicate the contributions of the three relaxation modes.

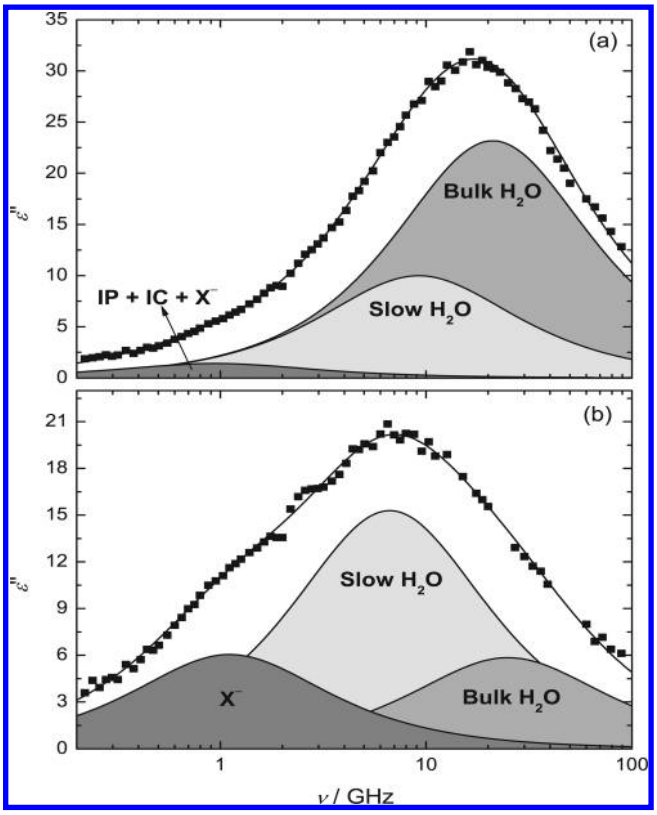

Figure 4. Dielectric loss curve of (a) 0.4867 M and (b) 2.770 M NaOBu(aq) at 25 °C, showing the contributions of the three Debye processes. Symbols represent experimental data, lines represent the D +D+D fit, and shaded areas indicate the contributions of the three relaxation modes.

which arises from the cooperative relaxation of its H-bond network.[32] This mode therefore can be assigned unequivocally to the relaxation of water molecules that are not significantly influenced by the presence of the solute particles. The value of τ_b decreases with increasing electrolyte concentration for both sets of solutions, which indicates that the ions influence the dynamics of water beyond their hydration shell(s). It should be noted that Longinova et al.[37] reported an increase in the bulk water relaxation time with increasing concentration in aqueous solutions of KOPr(aq). However, their measurements were restricted to a limited number and range of frequencies (just eight frequencies between 10 and 25 GHz) and consequently their data were fitted to a single Cole−Cole equation. The present spectra clearly indicate that there is more than one process in this frequency range, which suggests that the increase in τ_b reported by Longinova et al. may be a consequence of their inability to resolve the bulk and slow water modes.

The variation of τ_b with solute concentration was fitted by the empirical function

$$\tau_b(c) = (\tau(0) - a) + a \exp(-bc) \quad (5)$$

where the pure water value, $\tau(0)$, was taken to be 8.32 ps.[38] The fits and parameter values obtained for NaOPr(aq) and NaOBu(aq) with eq 5 are shown in Figure 5 and Table S1 (Supporting Information) along with, for convenience, the equivalent information for aqueous solutions of NaOFm and NaOAc.[8] The decrease in $\tau_b(c)$ with increasing c declines systematically from NaOFm(aq) to NaOPr(aq). However, this trend is reversed with NaOBu(aq) for which the decrease in $\tau_b(c)$ is even greater than for NaOFm(aq) (Figure 5). This is

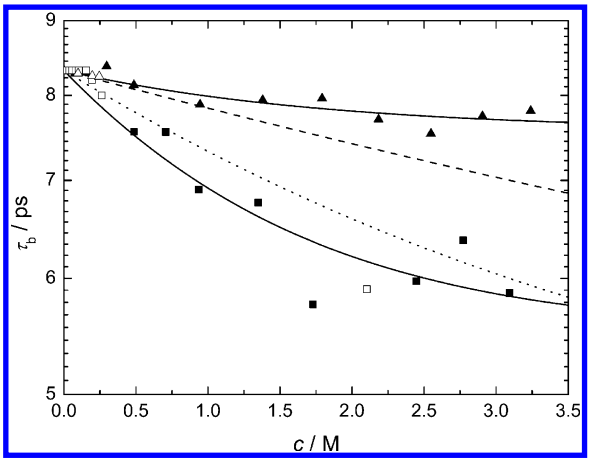

Figure 5. Solute-concentration dependence of the bulk water relaxation time, τ_b, for NaOPr(aq) (▲, Δ) and NaOBu(aq) (■, □) at 25 °C. Open symbols were fixed during the fitting procedure; solid lines represent the fit using eq 5; dotted and dashed lines represent the fits[8] for NaOFm(aq) and NaOAc(aq), respectively, using eq 5.

presumably a reflection of the greater size and hydrophobicity of OBu^-, whose sodium salt is the smallest member of the *n*-akylcarboxylates considered to be a hydrotrope[39] (see also section 4.3).

Slow Water. The intermediate (j = 2) process, centered at ~8 GHz, was resolved in the DR spectra of both sets of solutions for all investigated c. The average relaxation times for NaOPr(aq) and NaOBu(aq) were 19 and 21 ps, respectively.

dx.doi.org/10.1021/jp310029c | J. Phys. Chem. B 2013, 117, 2142−2152

These values are very similar to the "slow-water" relaxation time reported previously for the aqueous solutions of a number of hydrophilic[40,41] and hydrophobic[42,43] salts and are so assigned here. For NaOPr(aq), τ_s increases slightly with increasing concentration, whereas for NaOBu(aq), τ_s first decreases (at $c \leq 0.5$ M) and then steadily increases (Figure 6).

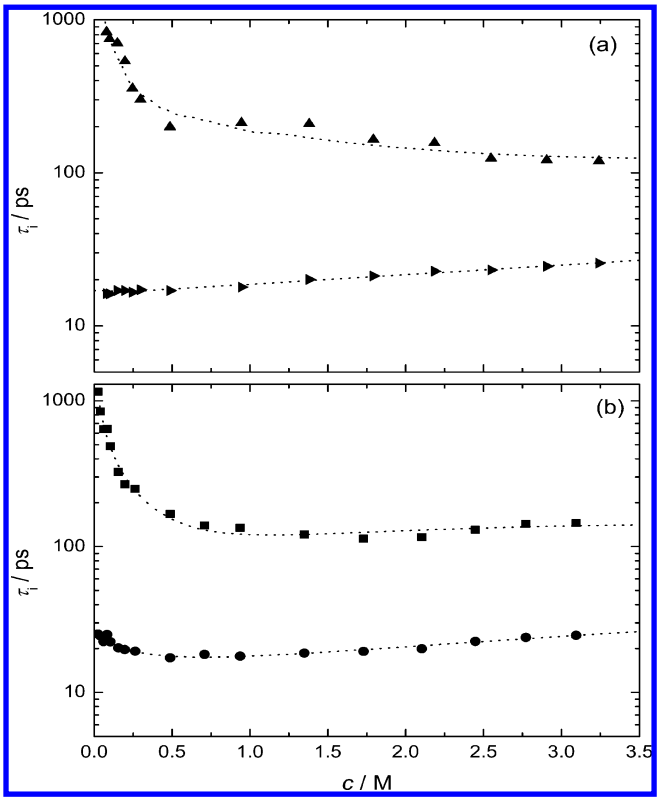

Figure 6. Solute-concentration dependence (a) for NaOPr(aq) of the solute relaxation time, τ_1 (▲) and slow water relaxation time, τ_s (▶) and (b) NaOBu(aq) of the solute relaxation time, τ_1 (■) and slow water relaxation time, τ_s (●) at 25 °C. Lines are a visual guide only.

Solute. The slowest ($j = 1$) process, centered at ~1 GHz for both NaOPr(aq) and NaOBu(aq), appears to be a composite. This conclusion is suggested by the very rapid decline in $\tau_1(c)$ as c increases up to ~0.5 M for both salts (Figure 6). This sharp decrease is consistent with the presence of an ion-cloud (IC) relaxation, known as the Debye–Falkenhagen effect,[44] and/or ion pairing.[45] Although the ion pairing of sodium carboxylate salts in aqueous solution is weak,[8,46] some indications of its existence have been found for NaOAc(aq)[8] and NaOAc-F_3(aq)[46] from DRS measurements and, for NaOAc(aq), from conductance[47] and potentiometric[48] studies. For NaOPr(aq) and NaOBu(aq) solutions, the presence of ion pairs (IPs) is strongly implied by the dramatic changes in the effective dipole moments derived from the DR data at low c (see section 4.5).

In addition to the IC and IP effects it must be remembered that OPr^- and OBu^- have permanent dipole moments, with calculated (MOPAC)[49] magnitudes of 5.9 and 8.4 D, respectively. As DRS is sensitive to all dipolar species present in solution these ions must contribute to the DR spectra. On the basis of their size, the rotational diffusion mode of OPr^-(aq) and OBu^-(aq) would be expected to occur in approximately the same frequency range as the IC and IP relaxations.

In summary, the observed low frequency mode centered at ~1 GHz probably contains three concentration-dependent contributions: an IC relaxation process and the rotational diffusion modes of IPs and anions. The IC contribution to the this mode is probably small and is expected to decrease rapidly with increasing solute concentration.[44,46] The contribution to the relaxation time from the presence of IPs is more difficult to predict[45] because it depends on the nature of the species formed (whether contact or solvent-separated IPs) and their extent of formation, neither of which is known a priori. This contribution would, however, also be expected to decline significantly with c.[22] Thus, the leveling out of $\tau_1(c)$ at high c for both sets of salt solutions (Figure 6) implies that at $c \gtrsim 1$ M this mode arises almost exclusively from the rotational diffusion of OPr^-(aq) and OBu^-(aq). Support for this description of the $j = 1$ mode comes from the bias-free simulations which clearly show (Figures S1 and S2, Supporting Information) the presence of two modes at low c but only one, somewhat shifted, mode at high c. Note that for NaOFm(aq) and NaOAc(aq)[8] the anion-reorientation mode overlapped with the slow-water relaxation because of the smaller size of their anions.

4.3. Water Relaxation Amplitudes. *Bulk Water.* Relaxation amplitudes can be analyzed with the Cavell equation,[50] which relates the observed amplitude S_j to the effective dipole moment $\mu_{\mathrm{eff},j}$ of the molecular-level species responsible for that process

$$\frac{\varepsilon + (1 - \varepsilon)A_j}{\varepsilon} S_j = \frac{N_A c_j}{3k_B T \varepsilon_0} \mu_{\mathrm{eff},j}^{\ 2} \tag{6}$$

where N_A and k_B are the Avogadro and Boltzmann constants, T is the thermodynamic temperature, ε is the static permittivity, c_j is the molar concentration of the species j, and A_j accounts for the shape of the reaction field.[51]

As shown previously,[42] the bulk and fast-water relaxations (the latter not resolved in the present spectra but evidenced by the high fitted values for ε_∞) can be taken as lying on a continuum, such that the total bulk-water amplitude (peak area), $S_b = \varepsilon_3(c) - \varepsilon_\infty$, can be analyzed collectively. To do this, the value of $\varepsilon_\infty = 3.48$ obtained for pure water from dielectric measurements that included THz data[38] is used rather than the fit results given in Tables 1 and 2. The magnitude of S_b decreases strongly with increasing c before starting to level off at $c \gtrsim 1$ M (Figure 7). These results were combined with the solvent-normalized Cavell equation[42] to calculate an apparent (i.e, DRS-detected) concentration of bulk water, c_w^{ap}. Kinetic depolarization effects,[28,52] due to the coupling of solvent-dipole reorientations and ion translation in the oscillating electromagnetic field, were accounted for by assuming "slip" boundary conditions.[28,53]

Slow Water. The amplitude of the slow-water process, S_s, for both sets of solutions initially increases strongly with increasing c (Figure 7), but eventually passes through a maximum at ~1.7 M for NaOBu(aq) and ~2.6 M (barely discernible) for NaOPr(aq). The former concentration coincides approximately with the concentrations at which OBu^- anions have been reported[54] to start aggregating in aqueous solution and where apparent molar volumes (V_ϕ) and especially heat capacities ($C_{p\phi}$) of NaOBu(aq) show anomalies.[55] While the effects are less marked for NaOPr(aq) the similarity of the trends in S_s (Figure 7) and in its V_ϕ and $C_{p\phi}$ values[55] suggest that some aggregation also occurs in these solutions. Consistent with its

dx.doi.org/10.1021/jp310029c | J. Phys. Chem. B 2013, 117, 2142–2152

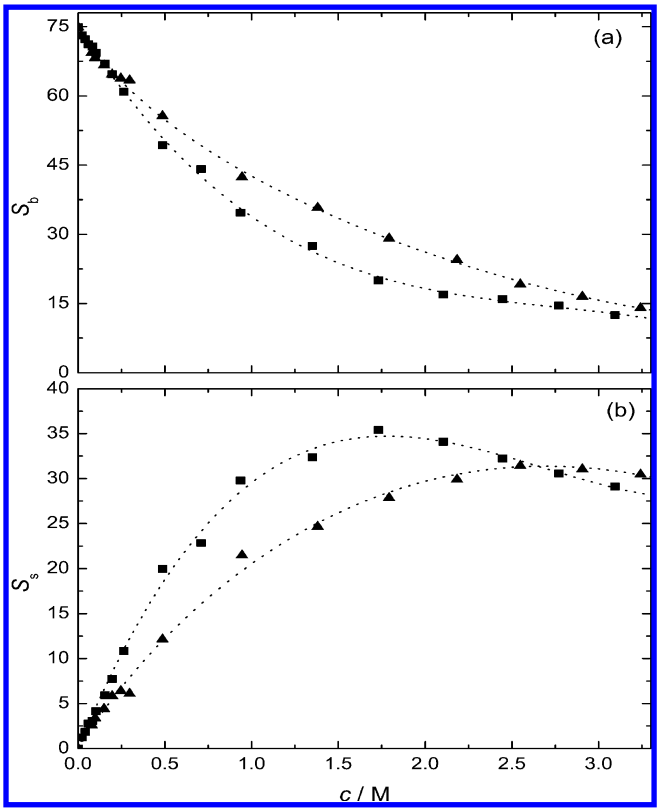

Figure 7. Solute-concentration dependence of (a) the bulk water relaxation amplitude, S_b, and (b) the slow water relaxation amplitude, S_s, for NaOPr(aq) (▲) and NaOBu(aq) (■) at 25 °C. Lines are a visual guide only.

shorter chain length these effects occur at higher concentrations than for NaOBu(aq).

4.4. Ion Hydration. As described by Buchner and Hefter,[22] the effects of ion solvation on DR spectra manifest themselves in three major ways: (a) a generalized shift of the solvent relaxation time, τ_S (subscript "S" for solvent), without a significant change of shape in the overall solvent mode, (b) a decrease of the solvent amplitude, S_S, and (c) the possible emergence of a new relaxation process arising from specific solvent molecules whose dynamics have been significantly perturbed by the presence of the dissolved ions. All these effects can be observed in the spectra of both of the present sets of solutions. Thus there is a decrease in the bulk-water relaxation time, τ_b (Figure 5), a strong decrease of bulk-water amplitude, S_b (Figure 7), and the emergence of a slow-water relaxation process, S_s (subscript "s" for slow, Figures 3 and 4) with increasing salt concentration.

If ion−water interactions are much stronger than water−water interactions, the water molecules bound to the ions become immobilized ("irrotationally-bound", ib) on the DR time scale and no longer contribute to the spectrum.[22] This leads to a decrease in the bulk-water relaxation amplitude, S_b. The difference between the analytical (total) water concentration, c_w, and the apparent value detected by DRS, c_w^{ap}, calculated from eq 6 and corrected for the amount of "slow" water, c_s^{ap}, can therefore be ascribed to the presence of such ib water molecules. An effective ib hydration number, Z_{ib}, can then be defined as number of such immobilized molecules per unit of solute

$$Z_{ib} = \frac{c_w - c_w^{ap} - c_s^{ap}}{c} \quad (7)$$

The Z_{ib} values so obtained (Figure 8) for NaOPr(aq) and NaOBu(aq) are either smaller or about the same as the number

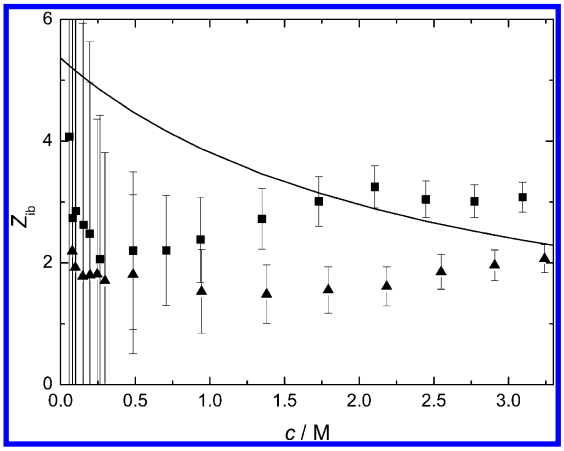

Figure 8. Concentration dependence of the number of irrotationally bound water molecules per solute unit, Z_{ib}, for NaOPr(aq) (▲) and NaOBu(aq) (■) at 25 °C.[53] Error bars are one standard deviation of the fit of the empirical equation: $S_b(c) = S_b(0)[= 78.37 - 3.48] + a_1c + a_2c^{3/2}$. The solid line represents $Z_{ib}(Na^+)$.[44]

of ib water molecules known to be associated with Na^+(aq) from DRS measurements on other sodium salt solutions.[44] Assuming ionic additivity this indicates that $Z_{ib} \approx 0$ for both OPr^-(aq) and OBu^-(aq). This result is consistent with the results obtained by DRS for OFm^-(aq) and OAc^-(aq)[8] and also for some dicarboxylate ions.[40] The small values of Z_{ib}(NaOPr) and Z_{ib}(NaOBu) at $c \gtrsim 1$ M (Figure 8) are implausible as they are less than $Z_{ib}(Na^+)$;[44] and this anomaly persists even at infinite dilution where strict ionic additivity of Z_{ib} should prevail. Given the very large uncertainties in Z_{ib} at low c (Figure 8) this apparent anomaly is more likely to be due to data fitting problems, especially given the composite nature of the overlapping $j = 1$ mode, rather than a real effect.

As already discussed (sections 4.2 and 4.3), the intermediate frequency ($j = 2$) process is due to the presence of slow water. The apparent concentration of slow water, $c_s^{ap}(c)$, which can be derived from the amplitude of this process, S_s, can be used to calculate the number of slowly relaxing water molecules per solute "molecule", Z_s

$$Z_s = \frac{c_s^{ap}}{c} \quad (8)$$

The Z_s values estimated for NaOPr(aq) and NaOBu(aq) with eq 8 are shown in Figure 9. Since the aqueous solutions of typical inorganic salts containing Na^+ do not show a slow water process,[28,44,56] these Z_s values can be assigned entirely to the anions. As these anions contain hydrophilic and hydrophobic moieties, both of which are known, from previous DRS studies,[8,40,46] MD simulations[15,57] and time-resolved IR spectroscopy,[58] to slow the dynamics of neighboring water molecules, it is reasonable to assume that

$$Z_s = Z_{hydrophilic} + Z_{hydrophobic} \quad (9)$$

If it is further assumed that these two effects operate independently, their respective contributions can be resolved as follows. The hydrophilic hydration of the carboxylate group

dx.doi.org/10.1021/jp310029c | J. Phys. Chem. B 2013, 117, 2142−2152

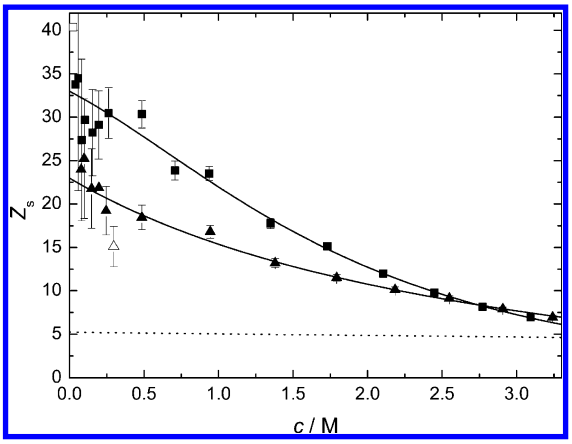

Figure 9. Concentration dependence of the number of slow water molecules per solute unit, Z_s, for $OPr^-(aq)$ (▲) and $OBu^-(aq)$ (■) at 25 °C. Error bars are one standard deviation of the fit of the empirical equation: $S_s(c) = a_1c + a_2c^{3/2}$. Solid lines represent fits with eq S1 (Supporting Information); the dotted line represents $Z_t(OFm^-(aq))$.[8] Open symbols are outliers that were not used in the fits.

($-COO^-$) can be estimated plausibly as $Z_s(OFm^-(aq))$ since formate has no hydrophobic component. This value, $Z_s(OFm^-(aq)) \approx Z_s(-COO^-(aq)) \approx 5.2$,[8] is independent of solute concentration and is remarkably similar to the Z_s values observed at high solute concentrations (see below) of other carboxylate ions including $OAc^-(aq)$ and $OAcF_3^-$ (aq) ($Z_s \approx 5$)[46] and even dicarboxylates such as malonate and succinate ($Z_s/2 \approx 5$ and 6, respectively).[40] This value also agrees satisfactorily with potentiometric measurements[59] which suggest ∼7 and ∼8.5 water molecules are hydrophilically bound to OPr^- and OBu^-, respectively.

The present infinite dilution values of Z_s of ∼23 and ∼33 water molecules for $OPr^-(aq)$ and $OBu^-(aq)$, respectively (Figure 9), are broadly consistent with the corresponding values[8] of $Z_s \approx 5.2$ and 11 for $OFm^-(aq)$ and $OAc^-(aq)$. That is, bearing in mind that the hydration of the carboxylate moiety is invariant, there is a marked systematic increase in $Z_{hydrophobic}$ with increasing alkyl chain length. The hydrophobic hydration of the alkyl chains of OPr^- and OBu^- is undoubtedly analogous that of well-recognized hydrophobic ions, such as the larger R_4N^+ cations ($R \geq$ *n*-Pr),[42] Ph_4P^+ and BPh_4^-.[43] The slower dynamics of the water molecules adjacent to such species is currently considered to be mainly due to shielding by the hydrophobic entity of those molecules from "fifth neighbour" attack, which is thought to control H-bond making and breaking.[42,60,61]

The pronounced decrease of Z_s with increasing solute concentration (Figure 9) is characteristic of hydrophobic hydration[42,43] and reflects the breakdown of the "fragile"[40] hydrophobic hydration sheaths due to a combination of overlapping (packing) effects, increasing solute−solute interactions and possibly anion aggregation (section 4.3). This confirms the assumption of the approximate constancy of the hydrophilic hydration of the $-COO^-$ group and supports the notion embodied in eq 9 of simple group additivity of slow water molecules, at least for the alkylcarboxylate ions.

It has been noted previously[8] that while hydrophobic hydration of the methyl group in the acetate ion ($H_3CCOO^-(aq)$) could be detected by DRS, no slow water was observed for the analogous tetramethylammonium ion ($(H_3C)_4N^+(aq)$).[42] The present results shed further light on this issue. Figure 10, which plots $Z_{hydrophobic}$ ($= Z_s - Z_{hydrophilic}$) for the $RCOO^-(aq)$ ions ($CH_3 \leq R \leq$ *n*-Pe) against the Z_s

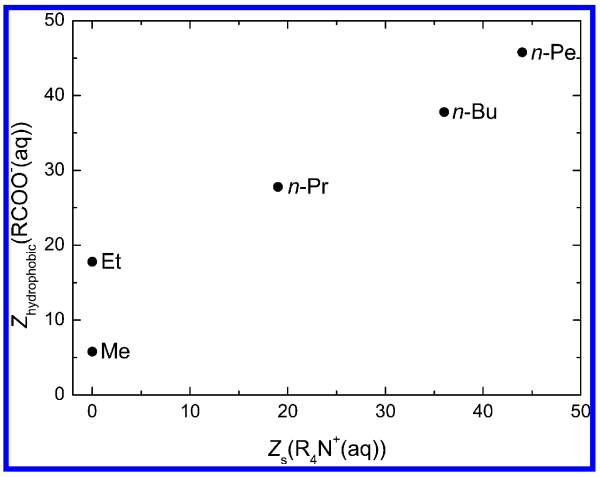

Figure 10. Correlation between $Z_{hydrophobic}$ for alkylcarboxylate ions ($RCOO^-(aq)$) and Z_s for the analogous tetraalkylammonium ions ($R_4N^+(aq)$)[42] at 25 °C.

values of the corresponding $R_4N^+(aq)$ ions[42] shows a very clear correlation between the two quantities. Of course it could be argued that the values of $Z_s(R_4N^+(aq))$ should be much larger because each tetraalkylammonium ion contains four hydrophobic entities. However, such a view ignores the structural difference between $RCOO^-$ and R_4N^+, with the alkyl moiety in the former being physically isolated from its charged (hydrophilic) part; the difference in the sign of the charge may also be important. But both of these factors are almost certainly outweighed by packing effects, because it has been noted that the values of $Z_s(R_4N^+(aq))$ are even smaller than would be expected from simple geometric considerations.[42] It would be of interest to compare the present correlation with the thermodynamic-probe method of Kondo et al., but there are insufficient data available at present.[62]

4.5. Solute Relaxation and Ion Association. As discussed above (Section 4.2), the slowest ($j = 1$) mode observed for both sets of solutions is a composite. Its amplitude, $S_1 = S_{IP} + S_{IC} + S_-$, for NaOPr(aq) passes through a maximum at $c \approx 0.2$ M before eventually increasing steadily at $c \gtrsim 1$ M (Figure 11). Broadly similar behavior is also observed for NaOBu(aq), with a poorly defined (barely discernible) maximum at $c \approx 0.1$ M followed by a steady increase at higher *c*. Given the present state of theoretical development it is not possible to allow for the IC relaxation contribution to the $j = 1$ mode but it is generally thought to be small and to decline rapidly with increasing *c*.[44] Consequently, and consistent with previous practice,[44,46] it was assumed that $S_{IC} \approx 0$ so that eq 6 could be used to calculate the effective dipole moment of the relaxing species, $\mu_{eff,1}$, from the observed magnitudes of S_1.

The presence of ion pairs at low *c* in both sets of solutions is indicated by the dramatic increase in $\mu_{eff,1}$ at $c \lesssim 0.5$ M (Figure 12). Similarly, the leveling out of $\mu_{eff,1}$ at higher *c* (Figure 12) is consistent with the predominance of the dipolar anions, which arises from the so-called redissociation of IPs.[22] These data can be used, following the procedures described in detail elsewhere,[63] to calculate values of the ion association constant, K_A. However, the K_A values so obtained from the present DRS data are at best upper limits, due to neglect of the (unknown) IC relaxation contribution, and are not well based because of the

dx.doi.org/10.1021/jp310029c | J. Phys. Chem. B 2013, 117, 2142−2152

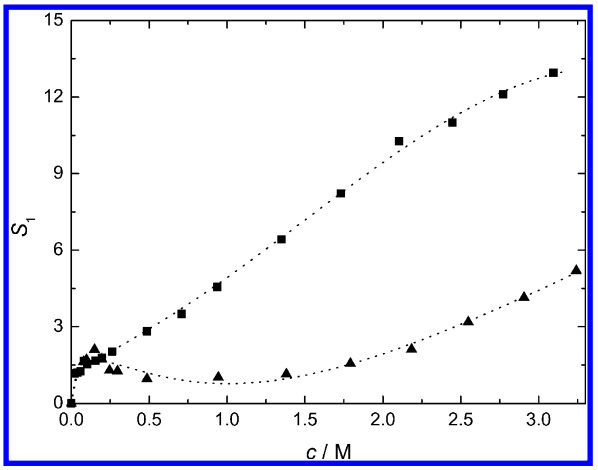

Figure 11. Concentration dependence of the solute-related relaxation amplitude, S_1, for NaOPr(aq) (▲) and NaOBu(aq) (■) at 25 °C. Lines are a visual guide only.

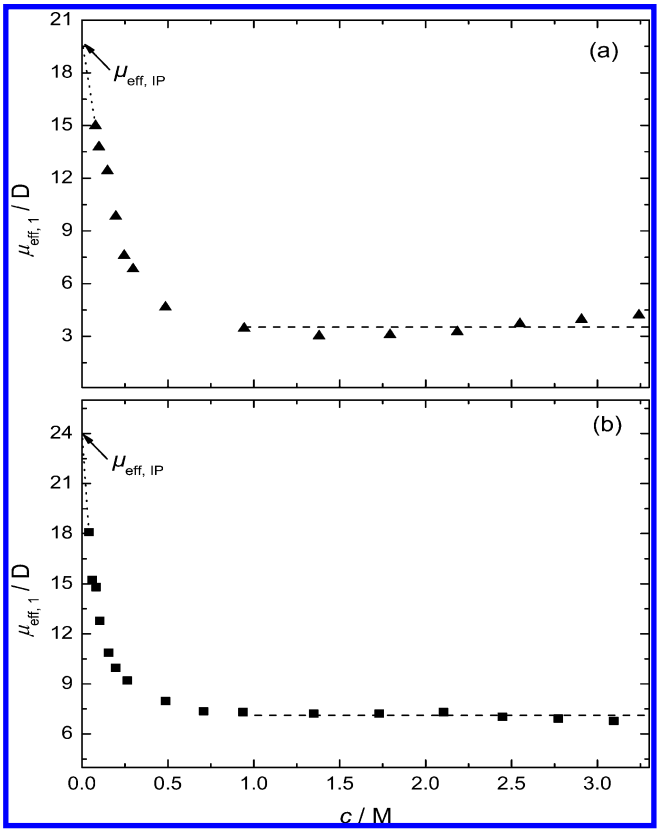

Figure 12. Concentration dependence of the effective dipole moment, $\mu_{eff,1}$, for j = 1 process calculated using the solute-related relaxation amplitude, S_1, for (a) NaOPr(aq) and (b) NaOBu(aq) at 25 °C. Dashed lines are averaged values of $\mu_{eff,-}$ for $RCOO^-(aq)$ at $c \gtrsim 1$ M; dotted lines are extrapolations to infinite dilution to obtain $\mu_{eff,IP}$.

many other assumptions involved in their derivation for these two systems. Accordingly, no numerical values are provided here. For completeness, however, further information on the calculation of such values is given along with a plot of K_A as a function of c (Figure S3) in the Supporting Information.

Although no quantitative results are presented, some qualitative comments on ion pairing in these solutions is appropriate. Given the fairly strong hydration of both Na^+ and the $RCOO^-$ ions it is reasonable to assume that any ion pairs formed by them will be solvent-separated and therefore fairly weak. No directly determined literature values are available for K_A of NaOPr(aq) and NaOBu(aq). However, using an equation analogous to that derived by Hefter,[64] and ignoring activity coefficient effects, values of $K_A \approx 0.06$ and 0.1 M^{-1} can be estimated for $NaOPr^0(aq)$ and $NaOBu^0(aq)$, respectively, in a 1 mol kg^{-1} KCl medium from the potentiometric pK_a measurements of Partanen and co-workers for propanoic[65] and butanoic[66] acids. These values are similar to those obtained for $NaOFm^0(aq)$ and $NaOAc^0(aq)$.[8] The lack of variation of the K_A values for the $[NaOOCR]^0(aq)$ ion pairs is not surprising given the similarity of the corresponding pK_a values but it is also consistent with the strong hydration of both Na^+ and the carboxylate ions leading to the formation of solvent-separated IPs. On this basis (see the Supporting Information), the values of K_A assuming solvent-shared IPs appear to be about 2 orders of magnitude too large. Even assuming the more physically realistic double solvent-separated IP (2SIP) structure, the K_A values are still possibly an order of magnitude too high. This suggests that at $c \lesssim 0.5$ M the contribution from ion-cloud relaxation to S_1 is not negligible for the present solutions.

5. CONCLUDING REMARKS

The present DRS results for NaOPr(aq) and NaOBu(aq) show that the anions OPr^- and OBu^- do not interact with water sufficiently strongly to cause significant irrotational bonding ($Z_{ib}(RCOO^-) \approx 0$) but do display both hydrophilic (of the $-COO^-$ moiety) and hydrophobic hydration (of the alkyl chain). Both types of interaction cause a slowing of the dynamics of neighboring water molecules; that is, they are responsible for the slow-water mode observed in the DR spectra (Figures 3 and 4). The clear emergence of a slow-water mode and the variation of its intensity (amplitude) with solute concentration (Figures 7b and 9) indicates that DRS is more sensitive to these types of hydration than IR spectroscopy since, for example, Stangret and co-workers[6] were unable to distinguish water molecules surrounding nonpolar groups from those in the bulk using that technique.

The hydrophobic and hydrophilic contributions to the slow-water mode can be separated by virtue of the strong dependence of the hydrophobic part, and independence of the hydrophilic part, on the solute concentration. Combination of the present results with previous DRS measurements[8] on NaOFm(aq) and NaOAc(aq) indicates a smooth increase in hydrophobic hydration with increasing alkyl chain length without significant change to the hydrophilic hydration of the $-COO^-$ group. The number of hydrophobically hydrated water molecules surrounding the $RCOO^-(aq)$ ions also correlates well with those reported for the corresponding $R_4N^+(aq)$ ions.

For NaOBu(aq), consistent with thermodynamic data[55] and its classification as a hydrotrope, the present DR spectra show features (e.g., Figure 7b) that point toward some form of aggregation at high solute concentrations ($c \gtrsim 1.7$ M). Similar effects, albeit smaller and at higher concentrations ($c \gtrsim 2.6$ M), were also detected for NaOPr(aq), which suggests that there is a more-or-less smooth transition toward hydrotropic behavior with increasing alkyl chain length rather than any sharp change at NaOBu(aq). In this context measurements on longer-chain alkylcarboxylates[67] will be of interest.

The low intensity mode centered at ~1 GHz in both sets of solutions provided evidence of weak association of the $Na^+(aq)$

dx.doi.org/10.1021/jp310029c | J. Phys. Chem. B 2013, 117, 2142−2152

and $RCOO^-(aq)$ ions, probably as 2SIPs but reliable estimates of the association constant could not be obtained because of the composite nature of this mode.

■ ASSOCIATED CONTENT

Supporting Information

Ion pairing calculations and additional figures illustrating data analysis and interpretation. This material is available free of charge via the Internet at http://pubs.acs.org.

■ AUTHOR INFORMATION

Corresponding Author

*E-mail: Richard.Buchner@chemie.uni-regensburg.de.

Notes

The authors declare no competing financial interest.

■ ACKNOWLEDGMENTS

The authors thank W. Kunz for the provision of laboratory facilities at Regensburg and S. Schrödle for recording VNA data for NaOPr(aq) at Murdoch University, Australia. The Higher Education Commission (HEC) of Pakistan is gratefully acknowledged for funding HMAR's stay in Germany. This work was funded by the Deutsche Forschungsgemeinschaft.

■ REFERENCES

(1) Bellisent-Funel, M.-C., Ed.; *Hydration Processes in Biology*; IOS Press: Dordrecht, The Netherlands, 1998.

(2) Kunz, W., Ed.; *Specific Ion Effects*; World Scientific: Singapore, 2010.

(3) Bakker, H. J. Structural Dynamics of Aqueous Salt Solutions. *Chem. Rev.* **2008**, *108*, 1456−1473.

(4) Marcus, Y. Effect of Ions on the Structure of Water: Structure Making and Breaking. *Chem. Rev.* **2009**, *109*, 1346−1370.

(5) Fayer, M. D. Dynamics of Water Interacting with Interfaces, Molecules, and Ions. *Acc. Chem. Res.* **2012**, *45*, 3−14.

(6) Gojło, E.; Śmiechowski, M.; Panuszko, A.; Stangret, J. Hydration of Carboxylate Anions: Infrared Spectroscopy of Aqueous Solutions. *J. Phys. Chem. B* **2009**, *113*, 8128−8136 and references cited therein.

(7) Laage, D.; Stirnemann, G.; Sterpone, F.; Rey, R.; Hynes, J. T. Reorientation and Allied Dynamics in Water and Aqueous Solutions. *Annu. Rev. Phys. Chem.* **2011**, *62*, 395−416.

(8) Rahman, H. M. A.; Hefter, G.; Buchner, R. Hydration of Formate and Acetate Ions by Dielectric Relaxation Spectroscopy. *J. Phys. Chem. B* **2012**, *116*, 314−323.

(9) Liang, T.; Walsh, T. R. Molecular Dynamics Simulations of Peptide Carboxylate Hydration. *Phys. Chem. Chem. Phys.* **2006**, *8*, 4410−4419.

(10) Campo, M. G. Molecular Dynamics Simulation of Glycine Zwitterion in Aqueous Solution. *J. Chem. Phys.* **2006**, *125*, 114511.

(11) Kameda, Y.; Sugawara, K.; Usuki, T.; Uemura, O. Hydration Structure of Alanine Molecule in Concentrated Aqueous Solutions. *Bull. Soc. Chem. Jpn.* **2003**, *76*, 935−943.

(12) McLain, S. E.; Soper, A. K.; Terry, A. E.; Watts, A. Structure and Hydration of L-Proline in Aqueous Solutions. *J. Phys. Chem. B* **2007**, *111*, 4568−4580.

(13) Wyttenbach, T.; Bowers, M. G. Hydration of Biomolecules. *Chem. Phys. Lett.* **2009**, *480*, 1−16.

(14) Beveridge, A. J.; Heywood, G. C. A Quantum Mechanical Study of the Active Site of Aspartic Proteinases. *Biochemistry* **1993**, *32*, 3325−3333.

(15) Payaka, A.; Tongraar, A.; Rode, B. M. QM/MM Dynamics of CH_3COO^-−Water Hydrogen Bonds in Aqueous Solution. *J. Phys. Chem. A* **2010**, *114*, 10443−10453 and references cited therein.

(16) Kuntz, I. D. Hydration of Macromolecules. III. Hydration of Polypeptides. *J. Am. Chem. Soc.* **1971**, *93*, 514−516.

(17) Kameda, Y.; Fukahara, K.; Mochiduki, K.; Naganuma, H.; Usuki, T.; Uemura, O. Structure of HCOOK Hydrated Melts. *J. Non-Cryst. Solids* **2002**, *312*−*314*, 433−437.

(18) Kameda, Y.; Mori, T.; Nishiyama, T.; Usuki, T.; Uemura, O. Structure of Concentrated Aqueous Sodium Formate Solutions. *Bull. Soc. Chem. Jpn.* **1996**, *69*, 1495−1504.

(19) Kameda, Y.; Ebata, H.; Usuki, T.; Uemura, O.; Misawa, M. Hydration Structure of Glycine Molecules in Concentrated Aqueous Solutions. *Bull. Soc. Chem. Jpn.* **1994**, *67*, 3159−3164.

(20) Jagoda-Cwiklik, B.; Vácha, R.; Lund, M.; Srebro, M.; Jungwirth, P. Ion Pairing as a Possible Clue for Discriminating between Sodium and Potassium in Biological and Other Complex Environments. *J. Phys. Chem. B* **2007**, *111*, 14077−14079.

(21) Hess, B.; Van der Vegt, N. F. A. Cation Specific Binding with Protein Surface Charges. *Proc. Natl. Acad. Sci. U.S.A.* **2009**, *106*, 13296−13300.

(22) Buchner, R.; Hefter, G. Interactions and Dynamics in Electrolyte Solutions by Dielectric Spectroscopy. *Phys. Chem. Chem. Phys.* **2009**, *11*, 8984−8999.

(23) Sato, T.; Buchner, R.; Fernandez, Š.; Chiba, A.; Kunz, W. Dielectric Relaxation Spectroscopy of Aqueous Amino Acid Solutions: Dynamics and Interactions in Aqueous Glycine. *J. Mol. Liq.* **2005**, *117*, 93−98.

(24) Lide, D. R. *CRC-Handbook of Chemistry and Physics*; CRC Press: Boca Raton, FL, 2004.

(25) Shaukat, S.; Buchner, R. Densities, Viscosities [from (278.15 to 318.15) K], and Electrical Conductivities (at 298.15 K) of Aqueous Solutions of Choline Chloride and Chloro-Choline Chloride. *J. Chem. Eng. Data* **2011**, *56*, 4944−4949.

(26) Buchner, R.; Hefter, G.; May, P. M.; Sipos, P. Dielectric Relaxation of Dilute Aqueous NaOH, $NaAl(OH)_4$, and $NaB(OH)_4$. *J. Phys. Chem. B* **1999**, *103*, 11186−11190.

(27) Barthel, J.; Buchner, R.; Eberspächer, P. N.; Münsterer, M.; Stauber, J.; Wurm, B. Dielectric Relaxation Spectroscopy of Electrolyte Solutions. Recent Developments and Prospects. *J. Mol. Liq.* **1998**, *78*, 83−109.

(28) Buchner, R.; Hefter, G. T.; May, P. M. Dielectric Relaxation of Aqueous NaCl Solutions. *J. Phys. Chem. A* **1999**, *103*, 1−9.

(29) Gregory, A. P.; Clarke, R. N. Dielectric Metrology with Coaxial Sensors. *Meas. Sci. Technol.* **2007**, *18*, 1372−1386.

(30) Buchner, R.; Chen, T.; Hefter, G. Complexity in "Simple" Electrolyte Solutions: Ion Pairing in $MgSO_4(aq)$. *J. Phys. Chem. B* **2004**, *108*, 2365−2375.

(31) Böttcher, C. F. J.; Bordewijk, P. *Theory of Electrical Polarization*; Elsevier: Amsterdam, The Netherlands, 1978; Vol. 2.

(32) Fukasawa, T.; Sato, T.; Watanabe, J.; Hama, Y.; Kunz, W.; Buchner, R. Relation between Dielectric and Low-Frequency Raman Spectra of Hydrogen-Bond Liquids. *Phys. Rev. Lett.* **2005**, *95*, 197802.

(33) Bevington, P. R. *Data Reduction and Error Analysis for the Physical Sciences*; McGraw-Hill: New York, 1978.

(34) Böttcher, C. F. J. *Theory of Electrical Polarization*; Elsevier: Amsterdam, The Netherlands, 1973; Vol. 1.

(35) Zasetsky, A. Y.; Buchner, R. Quasi-Linear Least Squares and Computer Code for Numerical Evaluation of Relaxation Time Distribution from Broadband Dielectric Spectra. *J. Phys.: Condens. Matter* **2011**, *23*, 025903.

(36) Hunger, J.; Stoppa, A.; Schrödle, S.; Hefter, G. T.; Buchner, R. Temperature Dependence of the Dielectric Properties and Dynamics of Ionic Liquids. *ChemPhysChem* **2009**, *10*, 723−733.

(37) Loginova, D. V.; Lileev, A. S.; Lyashchenko, A. K.; Khar'kin, V. S. Dielectric Properties of Aqueous Potassium Propionate Solutions from 288 to 308 K. *Russ. J. Inorg. Chem.* **2003**, *48*, 335−340.

(38) Schrödle, S. Effects of Nonionic Surfactants and Related Compounds on the Cooperative and Molecular Dynamics of their Aqueous Solutions. Ph.D. Thesis, University of Regensburg: Regensburg, Germany, 2005.

(39) Srinivas, V.; Rodley, G. A.; Ravikumar, K.; Robinson, W. T.; Turnbull, M. M.; Balasubramanian, D. Molecular Organization in Hydrotrope Assemblies. *Langmuir* **1997**, *13*, 3235−3239.

(40) Tromans, A.; May, P. M.; Hefter, G.; Sato, T.; Buchner, R. Ion Pairing and Solvent Relaxation Processes in Aqueous Solutions of Sodium Malonate and Sodium Succinate. *J. Phys. Chem. B* **2004**, *108*, 13789−13795.
(41) Fedotova, M. V.; Kruchinin, S. E.; Rahman, H. M. A.; Buchner, R. Features of Ion Hydration and Association in Aqueous Rubidium Fluoride Solutions at Ambient Conditions. *J. Mol. Liq.* **2011**, *159*, 9−17.
(42) Buchner, R.; Hölzl, C.; Stauber, J.; Barthel, J. Dielectric Spectroscopy of Ion-Pairing and Hydration in Aqueous Tetra-*n*-Alkylammonium Halide Solutions. *Phys. Chem. Chem. Phys.* **2002**, *4*, 2169−2179.
(43) Wachter, W.; Buchner, R.; Hefter, G. Hydration of Tetraphenylphosphonium and Tetraphenylborate Ions by Dielectric Relaxation Spectroscopy. *J. Phys. Chem. B* **2006**, *110*, 5147−5154.
(44) Eiberweiser, A.; Buchner, R. Ion-Pair or Ion-Cloud Relaxation? On the Origin of Small-Amplitude Low-Frequency Relaxations of Weakly Associating Aqueous Electrolytes. *J. Mol. Liq.* **2012**, *176*, 52−59.
(45) Buchner, R.; Barthel, J. Kinetic Processes in the Liquid Phase Studied by High-Frequency Permittivity Measurements. *J. Mol. Liq.* **1995**, *63*, 55−75.
(46) Rahman, H. M. A.; Buchner, R. Hydration and Sodium-Ion Binding of Trifluoroacetate in Aqueous Solution. *J. Mol. Liq.* **2012**, *176*, 93−100.
(47) Bončina, M.; Apelblat, A.; Bešter-Rogač, M. Dilute Aqueous Solutions with Formate Ions: A Conductometric Study. *J. Chem. Eng. Data* **2010**, *55*, 1951−1957.
(48) Daniele, P. G.; Robertis, A. D.; Stefano, C. D.; Sammartano, S.; Rigano, C. On the Possibility of Determining the Thermodynamic Parameters for the Formation of Weak Complexes Using a Simple Model for the Dependence on Ionic Strength of Activity Coefficients: Na^+, K^+, and Ca^{2+} Complexes of Low Molecular Weight Ligands in Aqueous Solution. *J. Chem. Soc., Dalton Trans.* **1985**, 2353−2361.
(49) Stewart, J. J. P. MOPAC 2009; *Stewart Computational Chemistry*, Version 9.341W, http://OpenMOPAC.net.
(50) Cavell, E. A. S.; Knight, P. C.; Sheikh, M. A. Dielectric Relaxation in Nonaqueous Solutions. Part 2. Solutions of Tri(*n*-butyl)ammonium Picrate and Iodide in Polar Solvents. *Trans. Faraday Soc.* **1971**, *67*, 2225−2233.
(51) Buchner, R.; Capewell, S. G.; Hefter, G. T.; May, P. M. Ion-Pair and Solvent Relaxation Processes in Aq. Na_2SO_4 solutions. *J. Phys. Chem. B* **1999**, *103*, 1185−1192.
(52) Hubbard, J. B.; Onsager, L. Dielectric Dispersion and Dielectric Friction in Electrolyte Solutions. I. *J. Chem. Phys.* **1977**, *67*, 4850−4857. (b) Hubbard, J. B. Dielectric Dispersion and Dielectric Friction in Electrolyte Solutions. II. *J. Chem. Phys.* **1978**, *68*, 1649−1664. (c) Hubbard, J. B.; Colonomos, P.; Wolynes, P. G. Molecular Theory of Solvated Ion Dynamics. III. The Kinetic Dielectric Decrement. *J. Chem. Phys.* **1979**, *71*, 2652−2661.
(53) The assumption of negligible kinetic depolarization yielded $Z_{ib} \approx 1...2$, whereas for stick boundary conditions $Z_{ib} \approx 3...4$ was obtained. In both cases the concentration dependence was similar to the slip results of Figure 8 and, as for slip, $Z_{ib}(\mathrm{NaOPr}) < Z_{ib}(\mathrm{NaOBu})$.
(54) Danielsson, I.; Stenius, P. Anion Association and Micelle Formation in Solutions of Hydrotropic and Short-Chain Carboxylates. *J. Colloid Interface Sci.* **1971**, *37*, 264−280.
(55) Bochmann, S.; May, P. M.; Hefter, G. Molar Volumes and Heat Capacities of Aqueous Solutions of Short-Chain Aliphatic Sodium Carboxylates at 25 °C. *J. Chem. Eng. Data* **2011**, *56*, 5081−5087.
(56) Wachter, W.; Kunz, W.; Buchner, R.; Hefter, G. Is There an Anionic Hofmeister Effect on Water Dynamics? Dielectric Spectroscopy of Aqueous Solutions of NaBr, NaI, $NaNO_3$, $NaClO_4$, and NaSCN. *J. Phys. Chem. A* **2005**, *109*, 8675−8683.
(57) Stirnemann, G.; Hynes, J. T.; Laage, D. Water Hydrogen Bond Dynamics in Aqueous Solutions of Amphiphiles. *J. Phys. Chem. B* **2010**, *114*, 3052−3059.
(58) Rezus, Y. L. A.; Bakker, H. J. Strong Slowing Down of Water Reorientation in Mixtures of Water and Tetramethylurea. *J. Phys. Chem. A* **2008**, *112*, 2355−2361.
(59) Backlund, S.; Eriksson, F.; Friman, R.; Rundt, K.; Sjöblom, J. Hydrophilic and Semihydrophilic Hydration of Short-Chain Ionic Surfactants. *Acta Chem. Scand. A* **1980**, *34*, 381−387.
(60) Kaatze, U.; Behrends, R.; Pottel, R. Hydrogen Network Fluctuations and Dielectric Spectrometry of Liquids. *J. Non-Cryst. Solids* **2002**, *305*, 19−28.
(61) Laage, D.; Hynes, J. T. A Molecular Jump Mechanism of Water Reorientation. *Science* **2006**, *311*, 832−835.
(62) Kondo, T.; Miyazaki, Y.; Inaba, A.; Koga, Y. Effects of Carboxylate Anions on the Molecular Organization of H_2O as Probed by 1-Propanol. *J. Phys. Chem. B* **2012**, *116*, 3571−3577.
(63) Barthel, J.; Hetzenauer, H.; Buchner, R. Dielectric Relaxation of Aqueous Electrolyte Solutions. II. Ion-Pair Relaxation of 1:2, 2:1, and 2:2 Electrolytes. *Ber. Bunsen Ges. Phys. Chem.* **1992**, *96*, 1424−1432.
(64) Hefter, G. T. Use of Lithium Perchlorate Media in the Study of Protolytic Equilibria. *J. Solution Chem.* **1984**, *13*, 179−190.
(65) Partanen, J. I.; Juusola, P. M.; Minkkinen, P. O. Determination of Stoichiometric Dissociation Constants for Propionic Acid in Aqueous Sodium or Potassium Chloride Solutions at 298.15 K. *Acta Chem. Scand.* **1999**, *53*, 547−556.
(66) Partanen, J. I.; Juusola, P. M. Determination of Stoichiometric Dissociation Constant of *n*-Butyric Acid in Aqueous Sodium or Potassium Chloride Solutions at 298.15 K. *Fluid Phase Equilib.* **2000**, *173*, 135−148.
(67) Rahman, H. M. A. Dielectric Spectroscopy of the Hydration of Organic Anions as Models for Anionic Residues of Biomolecules. Ph.D. Thesis, University of Regensburg: Regensburg, Germany, 2012.